Journal of Agriculture and Food Research 18 (2024) 101319

Contents lists available at ScienceDirect

Journal of Agriculture and Food Research

journal homepage: www.sciencedirect.com/journal/journal-of-agriculture-and-food-research

Estimation of botanical composition of forage crops using laboratory-based hyperspectral imaging and near-infrared spectrometer measurements

Junxiang Peng [a,*], Maryam Rahimi Jahangirlou [a,b], Julien Morel [c], Zhenjiang Zhou [d], David Parsons [a]

[a] Department of Crop Production Ecology, Swedish University of Agricultural Sciences, 90183 Umeå, Sweden
[b] Department of Agroecology, Aarhus University, 8830 Tjele, Denmark
[c] European Commission, Joint Research Centre, 21027 Ispra, Italy
[d] College of Biosystems Engineering and Food Science, Zhejiang University, 310058 Hangzhou, China

ARTICLE INFO

Keywords:
Forage
Botanical composition
Hyperspectral imaging
NIRS
Particle size

ABSTRACT

Harvested forage is the main raw feed for ruminant animals in Sweden, and is commonly cultivated in mixed stands of legume and grass species. The fraction of legume on a dry matter basis, known as botanical composition (BC) is a very important indicator of forage quality. In this study, hyperspectral imaging and near-infrared spectrometer (NIRS) based methods were used to estimate BC, to overcome the shortcomings of hand separation, which is time and resource consuming. Timothy and red clover mix samples were collected from different harvests in 2017–2019 from multiple sites in Northern Sweden and hand separated. The samples were synthetically mixed to 11 different BC levels, i.e., 0–100 % clover content. Two different instruments (Specim shortwave infrared (SWIR) hyperspectral imaging system and Foss 6500 spectrometer) were used to collect spectral data of samples milled to two levels of coarseness. Three different regression analyses: partial least squares regression (PLSR), support vector regression (SVR) and random forest regression (RFR), were used to build BC estimation models. The effects of the milling particle sizes and the different instruments on the performances of the models were compared. The data from second harvest in 2019 were used for independent validation as evaluation, and the rest of data were randomly split for model calibration (75 %) and validation (25 %). The models were iteratively run 1000 times with different splits, to check the effect from the splitting of calibration and validation datasets. Among different regression analyses, PLSR performed best, with mean Nash-Sutcliffe efficiency (*NSE*) for model evaluation from 0.76 to 0.87, varying for different instruments and milling sizes. Finer milling made the model accuracies slightly higher. This study developed quick and robust methods to determine the BC of timothy grass and red clover mixtures, which can provide useful information for farmers or researchers.

1. Introduction

In Sweden, forage grasslands occupy a greater proportion of agricultural lands than any other crop (44 % in 2022, [1]) and are the main feed source for ruminant animals. Forage quantity and quality are the main drivers of forage profitability and affect the efficiency of dairy and meat industries.

The main species of grass-legume mixed forage are timothy (*Phleum pratense* L.) and red clover (*Trifolium pratense* L.), and fields are typically harvested 3 to 4 times, depending on the latitude. Botanical composition (BC), is usually expressed as the proportion of clover or grass on a dry weight basis, in a mixed sward, and affects both biomass and quality of the forage [2,3]. BC varies among growing stages and harvests within the growing season, and it is highly associated with nitrogen fertilization requirements and forage quality. For example, Tessema et al. [4] found that the legume proportion was higher in non-fertilized ley fields compared to fields with nitrogen fertilization. Dindová et al. [5] reported that the increase of grass proportion increased the fibre content and yield of forage in the first harvest, whereas in the second and third harvests, increasing grass proportion improved the organic matter digestibility and net-energy for lactation. Determining BC accurately could help to recognize forage crop statuses, such as biomass, nitrogen

* Corresponding author.
E-mail address: junxiang.peng@slu.se (J. Peng).

https://doi.org/10.1016/j.jafr.2024.101319
Received 29 November 2023; Received in revised form 30 June 2024; Accepted 23 July 2024
Available online 24 July 2024

content and forage quality [4–8].

BC estimation in research studies is typically based on destructive field sampling and hand separation, which is time and resource consuming. Such methods are not appropriate for farming enterprises, and it is more typical for farmers to use visual assessments, which are not accurate and may not be representative of the whole field. It is typical for relevant stakeholders, such as scientists, advisors and farmers, to take samples from the field and mill them for forage quality analyses. A potential post-harvest BC determination method involves laboratory-based hyperspectral or near-infrared spectrometer (NIRS) scanning of milled samples, and could be an efficient tool to rapidly and accurately determine BC. Previous studies have reported the utilization of these types of instruments to estimate forage traits, such as using laboratory NIRS to detect legume-grass mixed forage quality [9], using laboratory and handheld NIRS to estimate lucerne-grass mixed forage nutritive values [10], and using laboratory NIRS and hyperspectral imaging to predict forage maize quality [11]. There are also several studies that focused on BC estimation using NIRS measurements, such as prediction of clover content in clover-grass mixed forage [12], prediction of the proportion of ryegrass, cocksfoot, tall fescue and clover in mixed forages [13], and BC estimation of lucerne-grass mixtures [14]. To the best of our knowledge, estimation of forage BC using hyperspectral imaging has not previously been tested. Furthermore, milling particle size, which affects sample surface scattering [15,16] and light absorption [17], has been reported to affect the performance of using mid-infrared spectroscopic analysis to estimate the plant leaf nutrient content [18], however its effect on BC prediction models has not been explored.

Partial least squares regression (PLSR) is commonly used to estimate crop nutritional characteristics with NIRS data [10,11,19] and BC [14]. PLSR has also been extensively used for *in situ* hyperspectral measurements for plant parameter estimation, such as cotton carotenoids [20], winter wheat leaf area index [21], tobacco photosynthetic capacity [22] and forage quality [23,24]. Moreover, several machine-learning based algorithms, such as support vector machine (SVM) and random forest (RF), are broadly applied for hyperspectral or NIRS data related classification or regression analyses; for example, nitrogen concentration estimation [25,26], wheat disease detection [27], and plant species classification [28,29].

The main research objective of this study was to build robust spectral data-based BC estimation models. Secondary objectives were to explore the effects of different spectral instruments and milling methods on the performances of the regression models.

2. Materials and methods

2.1. Field data collection

Field forage samples, which consisted of mixtures of grass (timothy; *Phleum pratense* L.) and legume (red clover; *Trifolium pratense* L.), were taken at several harvests (1st, 2nd and 3rd) between 2017 and 2019 from different fields at four sites (Ås, Lännäs, Öjebyn, and Röbäcksdalen) in Northern Sweden (Fig. 1).

A 76-cm diameter hoop was used to delineate 336 samples, which were cut and hand separated into grass and clover. The separated samples were oven dried at 60°C for 48 h to determine dry matter (DM) concentration and then BC was calculated. More detailed information on the samples is presented in Morel et al. [23] and Sun et al. [30]. Pairs of separated dried timothy and red clover samples in same treatment plots taken from 1st and 2nd harvests in 2017–2019 were manually re-combined to obtain synthetic samples with BC (expressed as percentage of red clover content, %) ranging from 0 to 100 %, with 10 % increments. Re-combined synthetic samples were then milled using a knife mill (SM300 Rostfrei, Retsch GmbH, Haan, Germany), through a 2-mm sieve, referred to as coarse milling. After the scanning of the milled samples using the hyperspectral and NIRS instruments, all of the milled samples were re-ground using a cyclone mill (Cyclotec 1093 sample, Foss Tecator, Höganäs, Sweden) with a 1-mm sieve, which pulverised samples to extremely small particles, referred to as fine milling. All of the samples were then rescanned using hyperspectral and NIRS instruments. Before scanning with hyperspectral and NIRS instruments, milled samples were placed in a fan-forced oven at 60°C for approximately 2 h to reduce and standardize the accumulated moisture. In total, 132 synthetic samples were created, spanning different locations, years, and harvests.

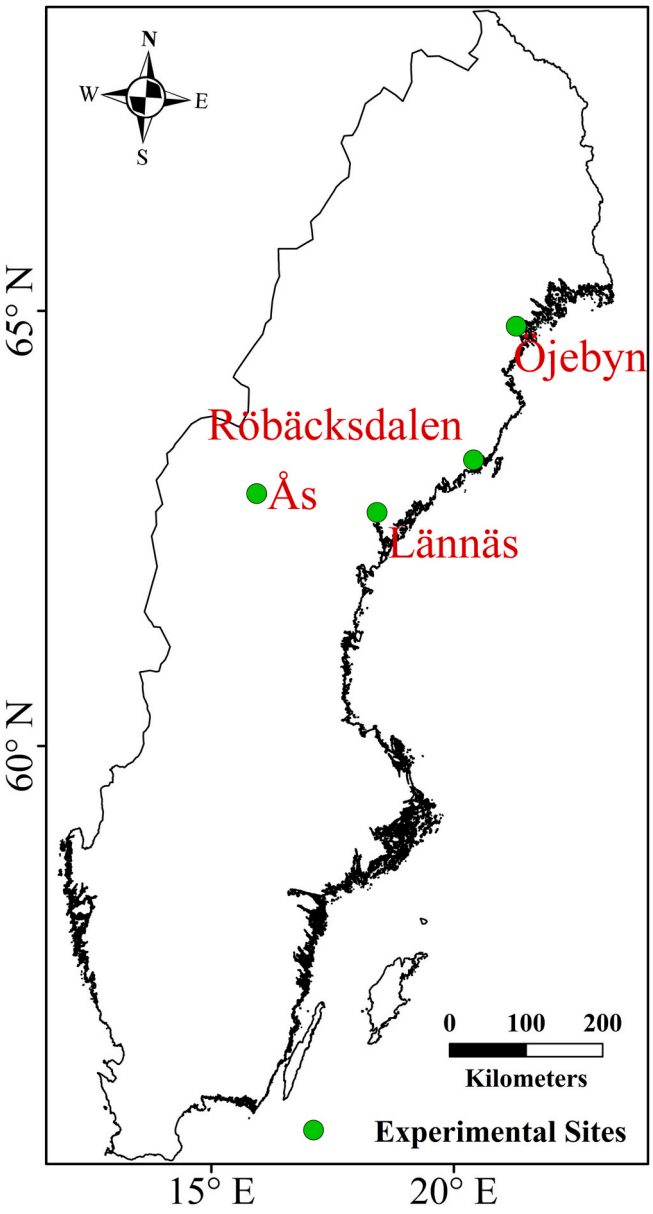

Fig. 1. Geographic locations of different sites in Sweden used in this study.

2.2. Spectral data acquisition

Spectral signatures were acquired using two laboratory instruments: (i) a NIR Foss 6500 spectrometer (Foss AS, Hillerød, Denmark) and (ii) a Specim shortwave infrared (SWIR) 3 hyperspectral camera (Specim, Spectral Imaging LTD., Oulu, Finland). The Foss spectrometer is a non-imaging system that measures the absorbed light spectrum from 400 to 2500 nm at 2 nm intervals. After the sensor calibration with a spectralon (Spectralon®, Labsphere Inc., Sutton, New Hampshire, USA) as white reference, each sample was filled into a spinning cup for scanning. After

each scanning, the sample was put back to its own container. For each sample, the scanning was replicated by refilling the spinning cup from the same milled samples. The Specim SWIR 3 instrument acquires hyperspectral images within the 1000–2495 nm spectral range, with a spectral interval of approximate 5.2 nm. The Specim SWIR 3 instrument was mounted on a machine (Umbio AB, Umeå, Sweden) which contains its own light source and movable platform. Before each sampling scanning, the shutter of the camera was closed to get the dark reference; afterwards the shutter was opened and the moveable platform was moved slightly forward to measure the incident light for getting the white reference. Then the same samples, placed in two Petri dishes as replicates, were moved forward with the moveable platform to scan the samples, after which the platform was moved backwards for the next scanning (See Fig. 2). The hyperspectral images were processed using Breeze software (Prediktera AB, Umeå, Sweden) to remove the background and export averaged absorbance spectra for samples in each Petri dish.

In order to reduce noise, 10 bands from the beginning and end of each instrument were removed and the remaining bands were used for the regression analyses. Following the spectral data control, two samples were removed from the analysis because of unexpected abnormal spectral signatures, and the remaining 130 samples were used for regression analyses.

2.3. Regression analyses

Before building multivariate regression models, which comprised PLSR, SVM based regression (support vector regression, SVR), and RF based regression (RFR) models, the sensitivity of each spectral band to the clover content was evaluated using univariate linear regressions in the R environment [31].

All of the multivariate regressions were tested in the R environment [31]. PLSR integrates principal component analysis and multiple linear regressions to decompose complex data matrices and correlate the predictor and response variables consequently so that only the most important linear combinations are utilized in the regression. The PLSR was run using the "*pls*" package [32] with a 10-fold cross-validation to optimize the number of principal components with minimum root mean squared error (RMSE). SVM allocates data from vector covariates into multidimensional feature space with kernel definition, where the linear regression can be implemented, therefore SVM can be used for regression analysis and the continuous output could be produced [33]. The SVR was operated using the "*e1071*" package [34], and the hyper-parameters (ε, C and γ [35]) were optimized based on a grid search with a radial basis kernel. ε is the function which could discipline prediction errors within the ±ε range. C is the parameter which determines the penalty weight of deviations outside ±ε. γ is a radial based kernel-specific parameter that contains the deviation between errors derived from the bias and variance in the adjusted model [24]. RF algorithm trains multiple different nonparametric trees using 2/3 of the samples (*in-bag*) and the rest 1/3 of the samples (*out-of-bag*) are used for internal cross-validation [36]. Once the different trees were trained, the averaging result from all of the trees is used as the final output from RF [37], and RF is able to run regression analysis (RFR, [38,39]). The "*RandomForest*" package was used to conduct RFR [40], and the '*tuneRF*' function was used to optimize the user-defined number of features (m_{try}), which is used to split nodes of each decision tree, and the parameter n_{tree}, user-defined number of trees for forest construction, was set at the default value of 500.

2.4. Model evaluation

The coefficient of determination (R^2) was used to evaluate the univariate linear analyses (i.e., band sensitivity analysis to BC and band collinearity analysis). For the multivariate regression analyses of BC estimation, the data from 2nd harvest in 2019 was used for independent evaluation, and the remaining data were randomly split for model calibration (75 %) and validation (25 %), respectively. For exploring the effect from the splitting of calibration and validation datasets, the models were iteratively run 1000 times with different splits.

The multivariate regression modelling accuracies were assessed using the Nash-Sutcliffe model efficiency (*NSE*), the Root Mean Square Error (*RMSE*), Ratio of Performance to Inter-Quartile distance (*RPIQ*) and bias [38,41], as described by equations (1)–(5), respectively.

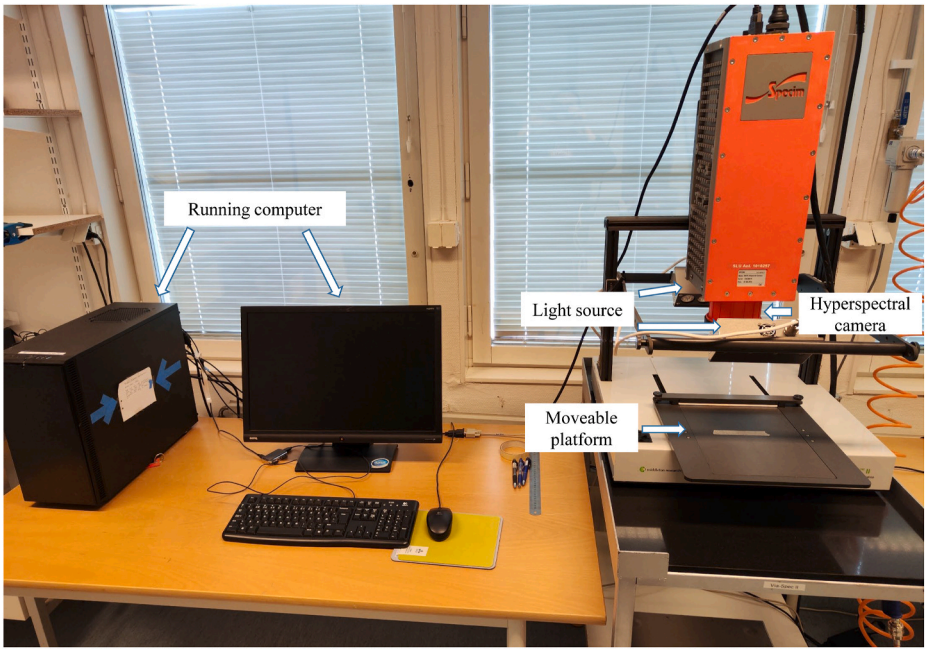

Fig. 2. Illustration of the hyperspectral imaging instrument containing Specim SWIR 3 camera, light source, moveable platform, and the running computer.

$$R^2 = \frac{\left(\sum_{i=1}^{n}(Sim_i - \overline{Sim})(Obs_i - \overline{Obs})\right)^2}{\sum_{i=1}^{n}(Sim_i - \overline{Sim})^2 \sum_{i=1}^{n}(Obs_i - \overline{Obs})^2} \quad (1)$$

$$NSE = 1 - \frac{\sum_{i=1}^{n}(Obs_i - Sim_i)^2}{\sum_{i=1}^{n}(Obs_i - \overline{Obs})^2} \quad (2)$$

$$RMSE = \sqrt{\frac{\sum_{i=1}^{n}(Obs_i - Sim_i)^2}{n}} \quad (3)$$

$$RPIQ = \frac{(Q3 - Q1)}{RMSE} \quad (4)$$

$$Bias = \frac{\sum_{i=1}^{n}(Obs_i - Sim_i)}{n} \quad (5)$$

Where Obs_i and Sim_i are observed and simulated values, $\overline{Obs}$ and $\overline{Sim}$ are mean observed and simulated values, and n is the total number of observations. Q1 and Q3 are the first and third quartiles of observed values. All of the calculations were implemented in R environment [31].

For evaluating the distributions patterns (e.g., absorbance over bands with different clover contents, *NSE* values derived from 1000 iterations), the mean and standard deviation values were computed in R environment using the functions "*mean*" and "*sd*" [31].

3. Results

3.1. Absorbance spectra

Table 1 shows the mean and standard deviations of absorbance spectra of coarse and fine milled samples as acquired from both instruments (Foss and Specim). The distributions of absorbance over bands with different clover contents (0, 50 % and 100 %) from two instruments (Foss and Specim) with different milling methods are illustrated in Fig. 3.

The samples with higher clover content tended to have higher overall absorbance values, especially for samples with coarse milling. The particle size also affected absorbance – mean and standard deviation values of absorbance from both instruments for coarse milled samples were higher than for fine milled samples. This indicated that fine milling reduced the spectral noise of sample absorbance compared to coarse milling. The differences of absorbance values between different clover content were greater with coarse milling than fine milling (mean values increased from 0.21 to 0.27 and 0.21 to 0.26 for Foss and Specim instruments with coarse milling, whereas mean values increased from 0.18 to 0.2 and 0.18 to 0.19 for Foss and Specim instruments with fine milling) (Table 1).

Table 1
Absorbance (mean ± standard deviation) for samples (coarse milling with 2-mm sieve or fine milling with 1-mm sieve) with different clover contents, scanned by different instruments (Foss and Specim).

Clover content (%)	Foss		Specim	
	Coarse Milled	Fine Milled	Coarse Milled	Fine Milled
0	0.21 ± 0.18	0.18 ± 0.16	0.21 ± 0.12	0.18 ± 0.10
10	0.21 ± 0.18	0.19 ± 0.16	0.21 ± 0.13	0.18 ± 0.10
20	0.22 ± 0.18	0.18 ± 0.16	0.22 ± 0.13	0.17 ± 0.09
30	0.22 ± 0.18	0.18 ± 0.16	0.22 ± 0.13	0.17 ± 0.10
40	0.22 ± 0.18	0.18 ± 0.16	0.23 ± 0.13	0.17 ± 0.09
50	0.23 ± 0.19	0.18 ± 0.17	0.23 ± 0.13	0.18 ± 0.10
60	0.24 ± 0.19	0.19 ± 0.17	0.24 ± 0.14	0.18 ± 0.10
70	0.25 ± 0.19	0.19 ± 0.17	0.25 ± 0.14	0.18 ± 0.10
80	0.25 ± 0.20	0.19 ± 0.17	0.25 ± 0.14	0.18 ± 0.11
90	0.26 ± 0.20	0.19 ± 0.18	0.25 ± 0.14	0.18 ± 0.11
100	0.27 ± 0.21	0.20 ± 0.17	0.26 ± 0.15	0.19 ± 0.11

3.2. Band sensitivity

The linear fits between absorbance values of each band with clover contents had overall poor performances ($R^2 < 0.5$, Fig. 4). The distributions of the fits accuracies from two different milling methods tended to follow similar patterns, yet a clear offset is evident, with higher R^2 values for the coarse milled samples. The spectral region between 1000 and 1450 nm responded differently, as R^2 values first increased from 1000 nm to 1300 nm and then decreased until 1450 nm for the fine milled samples, and the R^2 values were higher for the fine milled samples than for the coarse milled samples in the spectral region from 1200 nm to 1400 nm (Fig. 4). There was very little difference between the two different instruments at the same wavelengths (accuracies had similar values and distributions).

3.3. Model performance

Fig. 5 shows the distributions of the *NSE* values of model calibration, validation and evaluation calculated from the 1000 iterations with different random splitting of calibration and validation datasets. Table 2 further summarizes the distributions. Compared to the *NSE* values from model calibration (mean values range from 0.93 to 0.99, Table 2), the *NSE* values decreased for validation (mean values range from 0.58 to 0.97, Table 2) and evaluation (mean values range from −0.21 to 0.87, Table 2). The extent of the decrease depended on the model type, with the biggest drop for RFR, followed by SVR and PLSR. This could suggest an overfitting problem. Among different regression models, PLSR outperformed SVR and RFR with mean *NSE* values from iterative runs of 0.96–0.99, 0.89–0.97 and 0.76–0.87 for calibration, validation and evaluation (Table 2). The better performances of PLSR also translate into a smaller deviation for model validation and evaluation (Table 2) compared to SVR and RFR. This suggests that PLSR is more robust than SVR and RFR to estimate BC. Regarding the effect of milling methods, the coarse milling produced higher deviation of *NSE* values (Fig. 5, Table 2) compared to the fine milling, which indicates that the coarse milling made the modelling less stable with the iterative runs. The distributions of *NSE* values obtained with spectral data from the Foss and Specim instruments does not suggest any performance differences between the two instruments (Fig. 5, Table 2).

Table 3 provides a summary of the statistical indicators, derived from models with median calibration *NSE* values from the 1000 iterations with different instruments and milling methods (Fig. 5). Similar to results shown in Fig. 5, model calibration accuracies were high, with *NSE*, *RMSE*, *RPIQ* and bias ranging from 0.93 to 0.99, 2.8 %–8.41 %, 6.54 to 20.4, and −0.31 %–0.63 %. However, for the model validation, the accuracies declined as the range of *NSE*, *RMSE*, *RPIQ*, and bias varied between 0.62 and 0.98, 4.74 % and 19.89 %, 2.51 and 12.65 as well as −3.78 % and 2.9 %. Performances with the evaluation dataset showed obvious modelling differences. PLSR performed best, with ranges for the statistical indicators as follows: *NSE*, 0.78 to 0.85; *RMSE*, 12.27 %–14.8 %; *RPIQ*, 3.72 to 4.48, and bias, −5.25 %–10.05 %. RFR performed least effectively, with ranges of the statistical indicators as *NSE*, −0.17 to 0.42; *RMSE*, 24.18 %–34.21 %; *RPIQ*, 2.81 to 3.12; and bias, −14.83 and 26.7. SVR performed moderately with ranges of the statistical indicators as *NSE*, 0.62 to 0.69; *RMSE*, 17.6 %–19.58 %; *RPIQ*, 1.61 to 2.27; and bias, −7.02 %–10.74 %. Among these three regression algorithms, PLSR outperformed SVR and RFR, regardless of the instrument or the milling size. In contrast, RFR showed the poorest performance.

The effects of milling method on the model accuracy varied between instruments and algorithms (Table 3). Using the best performing algorithm, i.e., PLSR, as an example, the difference between coarse and fine

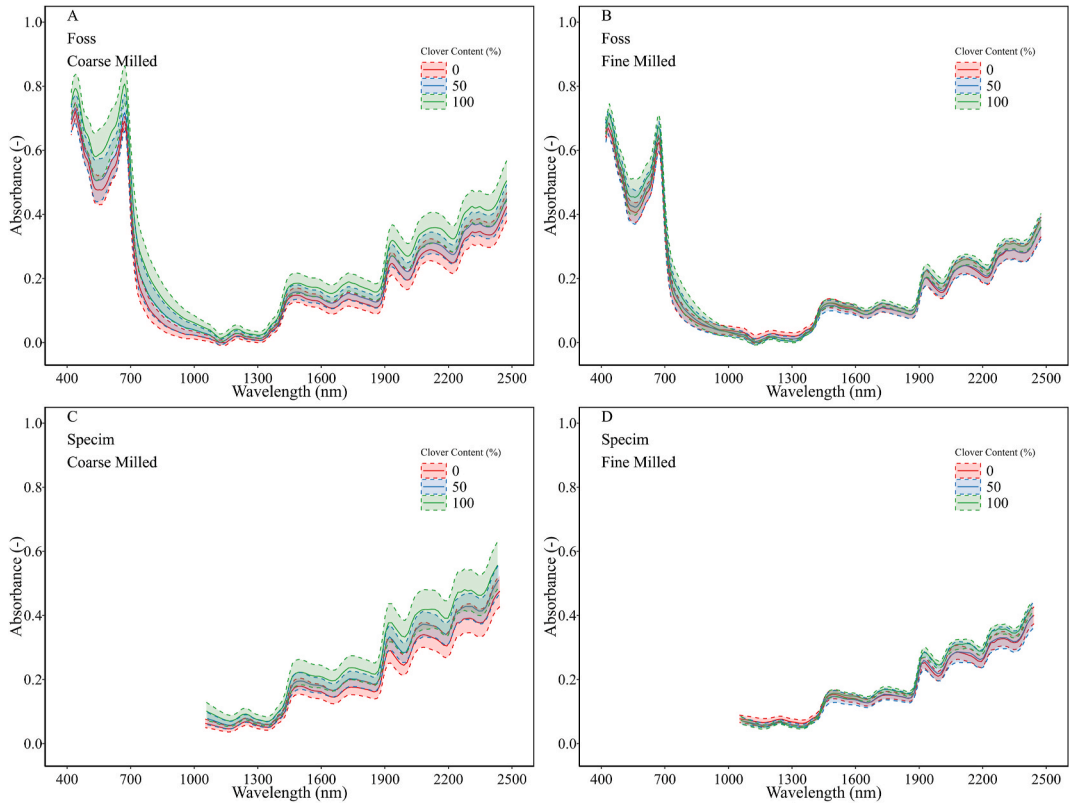

Fig. 3. Absorbance distributions over bands with different clover contents (0, 50 % and 100 %) from two instruments (Foss and Specim) with different milling methods (coarse milling with 2-mm sieve and fine milling with 1-mm sieve). The solid and dashed lines show mean and standard deviation of absorbance values.

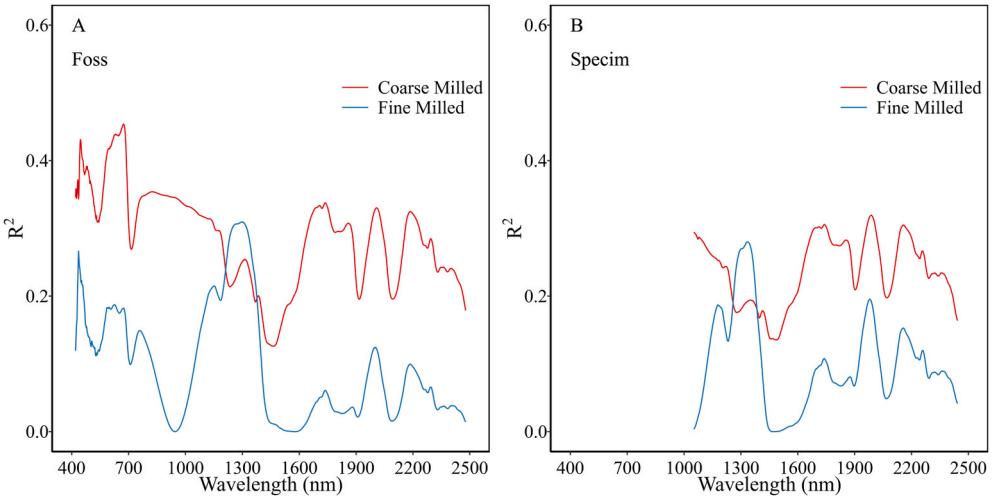

Fig. 4. Accuracies of linear correlations between absorbance values of each band and the clover contents, using data obtained from different instruments and milling methods.

milling methods was minor with the Foss, whereas there was clear difference with the Specim, where calibration accuracies increased (*NSE* and *RPIQ* values increased by 0.2 and 9.56, and *RMSE* values decreased by 3 %) from coarse milling to fine milling. The validation accuracies increased with fine milling as *NSE* increased from 0.83 to 0.98, *RPIQ* increased from 4.01 to 12.65, and *RMSE* declined from 12.74 % to 4.74 %. In contrast, the evaluation accuracies decreased with fine milling (*NSE* decreased from 0.85 to 0.78, *RPIQ* decreased from 4.48 to 3.72, and *RMSE* increased from 12.27 % to 14.8 %).

The accuracy of BC estimation was affected by the milling methods, the instruments, and the regression models. Overall, comparing different regression algorithms and milling methods, PLSR with fine milling performed best, based on its higher accuracy. The PLSR model results for Specim and Foss instruments with fine milling from Table 3 are shown in Fig. 6, and indicate that the difference in performances of Specim and Foss was minor.

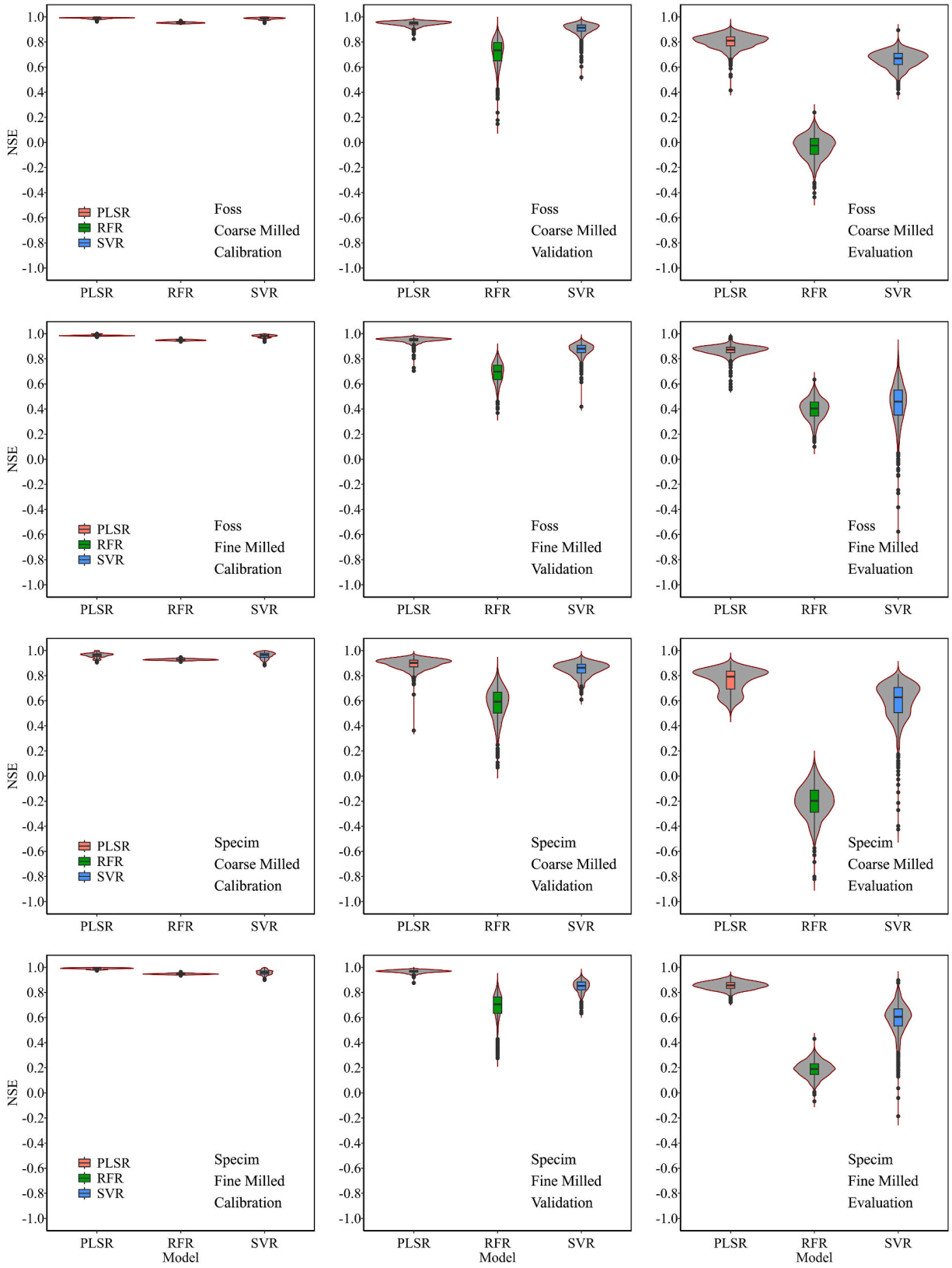

Fig. 5. Variations of Nash-Sutcliffe Efficiency (*NSE*) calculated from 1000 iterations using partial least squares regression (PLSR), random forest regression (RFR), and support vector regression (SVR) derived from spectral data obtained from a NIR Foss 6500 spectrometer and a Specim SWIR 3 hyperspectral camera, after either coarse milling or fine milling. The horizontal lines in each boxplot indicate the first quartile, median and third quartile of *NSE* values. The upper end of the black line is the upper bound for detecting outliers (Q3 + 1.5 × (Q3–Q1)) and the bottom end of the black line is the lower bound for detecting outliers (Q1 − 1.5 × (Q3–Q1)). Black dots represent outliers.

Table 2
Mean values and Standard deviations of Nash-Sutcliffe Efficiency (*NSE*) calculated from 1000 iterations using partial least squares regression (PLSR), random forest regression (RFR), and support vector regression (SVR) derived from spectral data obtained from different instruments (NIR Foss 6500 spectrometer and Specim SWIR 3 hyperspectral camera) and different milling methods (coarse milling and fine milling).

Instrument	Milling	Calibration			Validation			Evaluation		
		PLSR	RFR	SVR	PLSR	RFR	SVR	PLSR	RFR	SVR
Foss	*Coarse Milled*	0.99 ± 0.006	0.95 ± 0.005	0.99 ± 0.008	0.95 ± 0.02	0.71 ± 0.109	0.91 ± 0.046	0.8 ± 0.056	−0.04 ± 0.092	0.66 ± 0.067
	Fine Milled	0.99 ± 0.005	0.95 ± 0.004	0.98 ± 0.009	0.95 ± 0.023	0.69 ± 0.084	0.87 ± 0.048	0.87 ± 0.041	0.4 ± 0.084	0.44 ± 0.163
Specim	*Coarse Milled*	0.96 ± 0.018	0.93 ± 0.006	0.96 ± 0.023	0.89 ± 0.044	0.58 ± 0.128	0.85 ± 0.056	0.76 ± 0.093	−0.21 ± 0.133	0.59 ± 0.155
	Fine Milled	0.99 ± 0.005	0.95 ± 0.004	0.96 ± 0.018	0.97 ± 0.012	0.69 ± 0.102	0.85 ± 0.049	0.86 ± 0.033	0.19 ± 0.064	0.59 ± 0.126

Table 3
Statistical analysis results (*NSE*,*RMSE*, *RPIQ* and bias) for forage botanical composition (BC) estimation modelling derived from spectral data obtained from different instruments (NIR Foss 6500 spectrometer and Specim SWIR 3 hyperspectral camera) and different milling methods (coarse milling and fine milling) using partial least squares regression (PLSR), support vector regression (SVR), and random forest regression (RFR).

Instrument	Milling	Indicator	Calibration (n = 83)			Validation (n = 25)			Evaluation (n = 22)		
			PLSR	RFR	SVR	PLSR	RFR	SVR	PLSR	RFR	SVR
Foss	*Coarse Milled*	*NSE*	0.99	0.95	0.99	0.95	0.62	0.96	0.85	−0.17	0.63
		RMSE (%)	2.94	6.95	3.48	6.85	18.84	6.29	12.35	34.21	19.21
		RPIQ	20.40	17.24	8.63	7.30	9.55	3.19	4.45	2.86	1.61
		Bias (%)	0.00	−0.03	0.00	0.52	1.01	2.50	1.71	26.70	10.74
	Fine Milled	*NSE*	0.98	0.95	0.98	0.95	0.63	0.91	0.84	0.42	0.62
		RMSE (%)	3.95	7.05	4.03	6.74	19.89	9.80	12.50	24.18	19.58
		RPIQ	15.19	13.65	8.51	7.42	6.12	2.51	4.40	2.81	2.27
		Bias (%)	0.00	0.63	0.38	−1.09	−2.79	2.14	10.05	3.02	−1.83
Specim	*Coarse Milled*	*NSE*	0.97	0.93	0.97	0.83	0.63	0.91	0.85	−0.08	0.69
		RMSE (%)	5.93	8.41	5.82	12.47	19.52	9.66	12.27	32.82	17.60
		RPIQ	10.12	9.45	6.54	4.01	6.21	3.07	4.48	3.12	1.68
		Bias (%)	0.00	0.00	−0.28	0.47	−2.09	0.66	2.42	13.93	8.52
	Fine Milled	*NSE*	0.99	0.95	0.96	0.98	0.67	0.86	0.78	0.20	0.68
		RMSE(%)	2.80	7.22	6.44	4.74	18.45	11.30	14.80	28.21	17.86
		RPIQ	19.68	7.76	7.62	12.65	5.31	3.25	3.72	3.08	1.95
		Bias (%)	0.00	0.08	−0.31	−1.10	2.90	−3.78	−5.25	−14.83	−7.02

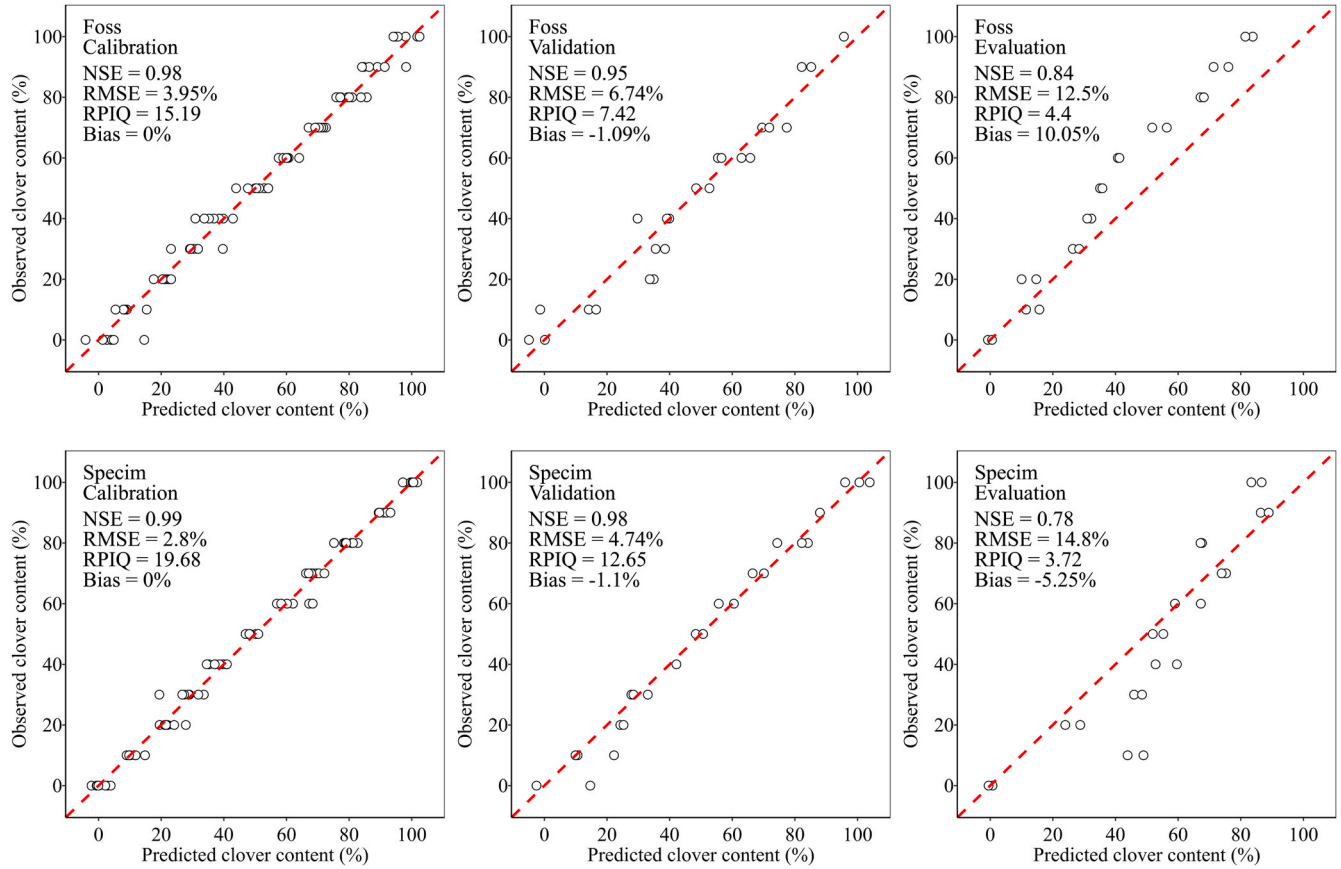

Fig. 6. Observed vs. estimated clover content for selected PLSR models with data from fine milled samples (Table 3).

4. Discussion

4.1. Sample absorbance patterns

In this study, samples with higher clover content had higher absorbance values. Red clover, and more generally legumes, usually absorbs more light than grasses because of pigmentation differences, i.e., clover plants have higher concentrations of light-absorbing pigments, such as chlorophyll, carotenoids and anthocyanins [42–44]. Because legumes can fix atmospheric nitrogen they typically have higher crude protein concentration than grasses [45]. One possible explanation why samples with higher clover content absorbed more light could be that after the drying and milling processes, these pigments were still functional, to a certain extent. These findings are confirmed by previous studies that explored the effect of different drying treatments on pigment contents of green plant leaves and showed that with oven drying at approximately 60°C, there was no obvious change in concentrations of chlorophyll and carotenoids, yet variations were reported among studied species [46,47]. Lewicki and Duszczyk [48] showed that the dehydrated leaves still absorb light after drying because of the preserved pigments. In this study, the absorbance differences among samples with different clover contents under coarse milling were larger, which might be because larger sized particles absorb more light, whereas smaller particles reflect more light [17].

4.2. Model performance

The regression modelling results (Fig. 5 and Table 2) show that PLSR performed better than SVR and RFR. Several other studies have also reported that PLSR outperformed other statistical methods such as SVR and even deep learning (DL) in the application of hyperspectral data [49]. PLSR links the spectral data and the target variables using a linear multivariate model by compressing and reducing the large number of collinear spectral variables to a few non-correlated latent variables with statistical determination of the relative contribution of the target variable to the spectral variables. PLSR also maximizes the correlation between the response and latent variables; hence it has strong ability to deal with dimensionality and noise in predictor variables [20,50,51]. Compared to other forage BC estimation models built from NIRS data using PLSR, the model accuracy from this study was similar to Chataigner et al. [13] and Karayilanli et al. [14], but higher than Wachendorf et al. [12]. In the current study, SVR performed similarly to PLSR, yet slightly poorer for the validation and evaluation subsets. Axelsson et al. [52] reported that SVR performance was weakened by

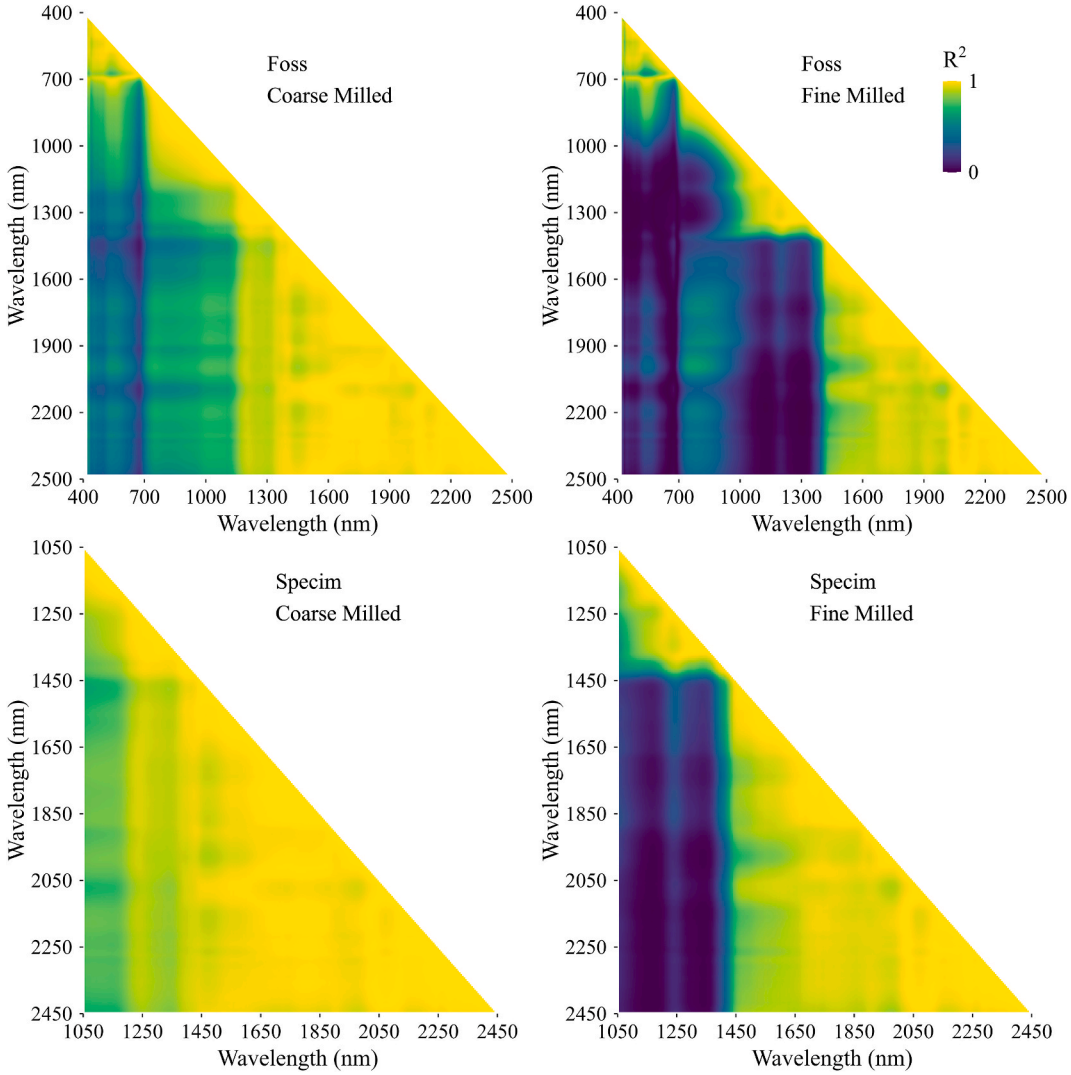

Fig. 7. The collinearity analysis between different bands. The values indicate the coefficient of determination (R^2) determined by linear fit between the absorbance of each band with the absorbance of all other bands for each instrument (Foss and Specim) and each milling method (coarse milling with a 2-mm sieve and fine milling with a 1-mm sieve).

multicollinearity if the full hyperspectral spectrum was used, and that selection of the most relevant bands should be conducted before running SVR. In addition to SVM based regression analyses, several other SVM based classification studies also reported that the feature selection can address the multicollinearity issue and, eventually, improve the performance of SVM [53–55]. In contrast to PLSR, RFR did not provide satisfactory results, especially for the validation and evaluation. Similar findings were recently reported by Morel et al [23] when using RFR for the prediction of forage quality parameters using *in situ* Yara-N sensor spectral data. The reason might be that RFR has difficulty extrapolating variables outside the range of its training datasets due to a poorer coverage ability (lower availability for data outside the training datasets range) derived from its relatively higher-level flexibility for non-linear relations fitting compared to other machine-learning algorithms, e.g., SVM [23,38]. This shortcoming tunes the RF model towards the training data and its predicted values rarely fall outside the training data range [56,57]. The high dimensionality of hyperspectral data might worsen the extrapolation problem. Several studies reported the challenge of using RF and hyperspectral data for classification purposes, due to the high dimensionality (and thus high multicollinearity) of the spectral data (e.g. Ref. [58,59]). Other studies propose selecting the most important variables by computing the variable importance scores before applying RF algorithms to improve modelling performance [60,61], which should be tested and applied in the future.

This study showed that finer milling led to more accurate modelling results. A possible reason is that finer milling reduces the noise (i.e., specularity) from the spectral data, as the particle size influences spectral signatures [62]. Fig. 7 shows that milling reduced the collinearity, represented by R^2 of linear fits between bands, e.g. 400–1400 nm and 1000–2500 nm for the Foss; and 1050–1400 nm and 1450–2450 nm for the Specim. Ikoyi and Younge [15] explored the effect of particle size on macro-mineral concentration estimation using NIRS spectrum and they found that model calibration accuracy was higher using data collected from milled dry hay samples with finer particle size. They explained that the reason could be that smaller particle size resulted in less spectral noise. However, considering practical applications, fine milling is less time and resource efficient compared to coarse milling, and the difference of performances related to the milling methods might not justify the use of fine milling samples. From a practical perspective, if a commercial laboratory was to offer a BC estimation service, the milling process should ideally be the same as for other forage quality analyses.

The difference of the performance between the instruments was not obvious– each has pros and cons. The Specim instrument has less bands, which could reduce the collinearity of input parameters. However, the Specim has an imaging sensor, in which imaging, processing, and data pre-processing are relatively time-consuming [11]. Foss has a non-imaging sensor, which needs less data pre-processing [10], but the data is relatively more redundant.

5. Conclusions

This study explored how well forage BC can be estimated by hyperspectral and NIRS data obtained from different instruments, different milling methods, and different regression algorithms. The main conclusions are:

(i) Samples with higher clover content had slightly higher absorbance values. Finer milling decreased this absorbance difference but also reduced the spectral noise.
(ii) Among different regression analyses for BC estimation, PLSR generally performed most optimally.
(iii) Overall, the regression modelling accuracies from data with finer milling were higher than for coarse milling.
(iv) There was no obvious accuracy difference between spectral instruments. However, processing of the data obtained from the Specim instrument requires more time and computation resources.

CRediT authorship contribution statement

Junxiang Peng: Writing – original draft, Software, Methodology, Investigation, Formal analysis, Data curation, Conceptualization. **Maryam Rahimi Jahangirlou:** Writing – review & editing, Methodology, Investigation, Data curation. **Julien Morel:** Writing – review & editing, Visualization, Supervision, Software, Resources, Project administration, Methodology, Investigation, Formal analysis, Data curation, Conceptualization. **Zhenjiang Zhou:** Writing – review & editing, Project administration, Methodology, Investigation, Funding acquisition, Data curation. **David Parsons:** Writing – review & editing, Visualization, Supervision, Resources, Project administration, Methodology, Investigation, Funding acquisition, Formal analysis, Conceptualization.

Declaration of competing interest

The authors declare that they have no known competing financial interests or personal relationships that could have appeared to influence the work reported in this paper.

Data availability

Data will be made available on request.

Acknowledgement

This study was supported by SLF (Stiftelsen Lantbruksforskning) and RJN (Regional Jordbruksforskning i Norra Sverige). Thanks are given to SLU (Sveriges lantbruksuniversitet) Röbäcksdalen field station and SITES (Swedish Infrastructure for Ecosystem Sciences) for the support of data collection and processing. The first author would like to thank Kempestiftelserna for funding of a postdoctoral scholarship.

References

[1] Jordbruksverket, 2022. Agricultural Statistics. (https://statistik.sjv.se/PXWeb/pxweb/sv/Jordbruksverkets%20statistikdatabas/?rxid=5adf4929-f548-4f27-9bc9-78e127837625). Accessed 2 November 2022. Swedish Board of Agriculture.
[2] K. Pirhofer-Walzl, K. Søegaard, H. Høgh-Jensen, J. Eriksen, M.A. Sanderson, J. Rasmussen, J. Rasmussen, Forage herbs improve mineral composition of grassland herbage, Grass Forage Sci. 66 (2011) 415–423.
[3] S. Ravetto Enri, M. Renna, M. Probo, C. Lussiana, L.M. Battaglini, M. Lonati, G. Lombardi, Relationships between botanical and chemical composition of forages: a multivariate approach to grasslands in the Western Italian Alps, J. Sci. Food Agric. 97 (2017) 1252–1259.
[4] Z. Tessema, A. Ashagre, M. Solomon, Botanical composition, yield and nutritional quality of grassland in relation to stages of harvesting and fertiliser application in the highlands of Ethiopia, Afr. J. Range Forage Sci. 27 (2010) 117–124.
[5] A. Dindová, J. Hakl, Z. Hrevušová, P. Nerušil, Relationships between long-term fertilization management and forage nutritive value in grasslands, Agric. Ecosyst. Environ. 279 (2019) 139–148.
[6] D. Andueza, A.M. Rodrigues, F. Picard, N. Rossignol, R. Baumont, U. Cecato, A. Farruggia, Relationships between botanical composition, yield and forage quality of permanent grasslands over the first growth cycle, Grass Forage Sci. 71 (2016) 366–378.
[7] Jordbruksverket, Rekommendationer för gödsling och kalkning 2023. https://webbutiken.jordbruksverket.se/sv/artiklar/jo219.html).SwedishBoardofAgriculture, 2022.
[8] K.M. Mercier, C.D. Teutsch, S.R. Smith, E.L. Ritchey, K.H. Burdine, E.S. Vanzant, Nitrogen fertilizer rate effects on yield and botanical components of summer annual forage mixtures, Agron. J. 113 (2021) 2798–2811.
[9] S. Biewer, T. Fricke, M. Wachendorf, Development of canopy reflectance models to predict forage quality of legume–grass mixtures, Crop Sci. 49 (2009) 1917–1926.
[10] M.F. Digman, J.H. Cherney, D.J.R. Cherney, The relative performance of a benchtop scanning monochromator and handheld fourier transform near-infrared reflectance spectrometer in predicting forage nutritive value, Sensors 22 (2022) 658.
[11] M. Hetta, Z. Mussadiq, J. Wallsten, M. Halling, C. Swensson, P. Geladi, Prediction of nutritive values, morphology and agronomic characteristics in forage maize using two applications of NIRS spectrometry, Acta Agric. Scand. Sect. B Soil Plant Sci 67 (2017) 326–333.

[12] M. Wachendorf, Ingwersen, F. Taube, Prediction of the clover content of red clover- and white clover-grass mixtures by near-infrared reflectance spectroscopy. Grass and Forage, Science 54 (2001) 87–90.
[13] F. Chataigner, F. Surault, C. Huyghe, B. Julier, Determination of Botanical Composition in Multispecies Forage Mixtures by Near Infrared Reflectance Spectroscopy. Sustainable Use of Genetic Diversity in Forage and Turf Breeding, Springer, 2010, pp. 199–203.
[14] E. Karayilanli, J.H. Cherney, P. Sirois, D. Kubinec, D.J.R. Cherney, Botanical composition prediction of alfalfa–grass mixtures using NIRS: developing a robust calibration, Crop Sci. 56 (2016) 3361–3366.
[15] A.Y. Ikoyi, B.A. Younge, Influence of forage particle size and residual moisture on near infrared reflectance spectroscopy (NIRS) calibration accuracy for macro-mineral determination, Anim. Feed Sci. Technol. 270 (2020) 114674.
[16] B. Reddersen, T. Fricke, M. Wachendorf, Effects of sample preparation and measurement standardization on the NIRS calibration quality of nitrogen, ash and NDFom content in extensive experimental grassland biomass, Anim. Feed Sci. Technol. 183 (2013) 77–85.
[17] Z. Sun, J. Zhang, Z. Tong, Y. Zhao, Particle size effects on the reflectance and negative polarization of light backscattered from natural surface particulate medium: soil and sand, J. Quant. Spectrosc. Radiat. Transf. 133 (2014) 1–12.
[18] C.R. Whatley, N.K. Wijewardane, R. Bheemanahalli, K.R. Reddy, Y. Lu, Effects of fine grinding on mid-infrared spectroscopic analysis of plant leaf nutrient content, Sci. Rep. 13 (2023) 6314.
[19] A.Y. Ikoyi, B.A. Younge, Faecal near-infrared reflectance spectroscopy profiling for the prediction of dietary nutritional characteristics for equines, Anim. Feed Sci. Technol. 290 (2022) 115363.
[20] Q. Yi, G. Jiapaer, J. Chen, A. Bao, F. Wang, Different units of measurement of carotenoids estimation in cotton using hyperspectral indices and partial least square regression, ISPRS J. Photogrammetry Remote Sens. 91 (2014) 72–84.
[21] X. Li, Y. Zhang, Y. Bao, J. Luo, X. Jin, X. Xu, X. Song, G. Yang, Exploring the best hyperspectral features for LAI estimation using partial least squares regression, Rem. Sens. 6 (2014) 6221–6241.
[22] K. Meacham-Hensold, C.M. Montes, J. Wu, K. Guan, P. Fu, E.A. Ainsworth, T. Pederson, C.E. Moore, K.L. Brown, C. Raines, High-throughput field phenotyping using hyperspectral reflectance and partial least squares regression (PLSR) reveals genetic modifications to photosynthetic capacity, Rem. Sens. Environ. 231 (2019) 111176.
[23] J. Morel, Z. Zhou, L. Monteiro, D. Parsons, Estimation of the nutritive value of grasslands with the Yara N-sensor field spectrometer, The Plant Phenome Journal 5 (2022) e20054.
[24] Z. Zhou, J. Morel, D. Parsons, S.V. Kucheryavskiy, A.-M. Gustavsson, Estimation of yield and quality of legume and grass mixtures using partial least squares and support vector machine analysis of spectral data, Comput. Electron. Agric. 162 (2019) 246–253.
[25] L. Liang, L. Di, T. Huang, J. Wang, L. Lin, L. Wang, M. Yang, Estimation of leaf nitrogen content in wheat using new hyperspectral indices and a random forest regression algorithm, Rem. Sens. 10 (2018) 1940.
[26] F. Wang, J. Huang, Y. Wang, Z. Liu, F. Zhang, Estimating nitrogen concentration in rape from hyperspectral data at canopy level using support vector machines, Precis. Agric. 14 (2013) 172–183.
[27] L. Huang, W. Ding, W. Liu, J. Zhao, W. Huang, C. Xu, D. Zhang, D. Liang, Identification of wheat powdery mildew using in-situ hyperspectral data and linear regression and support vector machines, J. Plant Pathol. 101 (2019) 1035–1045.
[28] J. Gao, D. Nuyttens, P. Lootens, Y. He, J.G. Pieters, Recognising weeds in a maize crop using a random forest machine-learning algorithm and near-infrared snapshot mosaic hyperspectral imagery, Biosyst. Eng. 170 (2018) 39–50.
[29] A. Sabat-Tomala, E. Raczko, B. Zagajewski, Comparison of support vector machine and random forest algorithms for invasive and expansive species classification using airborne hyperspectral data, Rem. Sens. 12 (2020) 516.
[30] S. Sun, Z. Zuo, W. Yue, J. Morel, D. Parsons, J. Liu, J. Peng, H. Cen, Y. He, J. Shi, X. Li, Z. Zhou, Estimation of biomass and nutritive value of grass and clover mixtures by analyzing spectral and crop height data using chemometric methods, Comput. Electron. Agric. 192 (2022) 106571.
[31] R Core Team, R: A Language and Environment for Statistical Computing, R Foundation for Statistical Computing, Vienna, Austria, 2022.
[32] B.-H. Mevik, R. Wehrens, The pls package: principal component and partial least squares regression in R, J. Stat. Software 18 (2007) 1–23.
[33] G. Mountrakis, J. Im, C. Ogole, Support vector machines in remote sensing: a review, ISPRS J. Photogrammetry Remote Sens. 66 (2011) 247–259.
[34] D. Meyer, E. Dimitriadou, K. Hornik, A. Weingessel, F. Leisch. e1071: Misc Functions of the Department of Statistics, Probability Theory Group (Formerly: E1071), TU Wien, 2023 version 1.7-14, https://CRAN.R-project.org/package=e1071.
[35] N. Cristianini, J. Shawe-Taylor, An Introduction to Support Vector Machines and Other Kernel-Based Learning Methods, Cambridge University Press, Cambridge, 2000.
[36] L. Breiman, Random forests, Machine Learning 45 (2001) 5–32.
[37] M. Belgiu, L. Drăguţ, Random forest in remote sensing: a review of applications and future directions, ISPRS J. Photogrammetry Remote Sens. 114 (2016) 24–31.
[38] J. Peng, K. Manevski, K. Kørup, R. Larsen, M.N. Andersen, Random forest regression results in accurate assessment of potato nitrogen status based on multispectral data from different platforms and the critical concentration approach, Field Crops Res. 268 (2021) 108158.
[39] S. Oliveira, F. Oehler, J. San-Miguel-Ayanz, A. Camia, J.M.C. Pereira, Modeling spatial patterns of fire occurrence in Mediterranean Europe using multiple regression and random forest, Forest Ecol. Manag. 275 (2012) 117–129.
[40] A. Liaw, M. Wiener, randomForest: breiman and Cutler's random forests for classification and regression, R package version 4 (2015) 14.
[41] V. Bellon-Maurel, E. Fernandez-Ahumada, B. Palagos, J.-M. Roger, A. McBratney, Critical review of chemometric indicators commonly used for assessing the quality of the prediction of soil attributes by NIR spectroscopy, TrAC Trends Anal. Chem. 29 (2010) 1073–1081.
[42] S. Dalmannsdottir, M. Rapacz, M. Jørgensen, L. Østrem, A. Larsen, R. Rødven, O. A. Rognli, Temperature before cold acclimation affects cold tolerance and photoacclimation in timothy (Phleum pratense L.), perennial ryegrass (lolium perenne L.) and red clover (Trifolium pratense L.), J. Agron. Crop Sci. 202 (2016) 320–330.
[43] J. De Majnik, J. Weinman, M. Djordjevic, B. Rolfe, G. Tanner, R. Joseph, P. Larkin, Anthocyanin regulatory gene expression in transgenic white clover can result in an altered pattern of pigmentation, Aust. J. Plant Physiol. 27 (2000) 659–667.
[44] A.M. Smith, T. Wang, The carotene content of certain species of grassland herbage, J. Agric. Sci. 31 (1941) 370–378.
[45] C. King, J. McEniry, M. Richardson, P. O'kiely, Yield and chemical composition of five common grassland species in response to nitrogen fertiliser application and phenological growth stage, Acta Agric. Scand. Sect. B Soil Plant Sci 62 (2012) 644–658.
[46] P.S. Negi, S.K. Roy, Effect of blanching and drying methods on β -carotene, ascorbic acid and chlorophyll retention of leafy vegetables, LWT - Food Sci. Technol. (Lebensmittel-Wissenschaft -Technol.) 33 (2000) 295–298.
[47] S. Roshanak, M. Rahimmalek, S.A.H. Goli, Evaluation of seven different drying treatments in respect to total flavonoid, phenolic, vitamin C content, chlorophyll, antioxidant activity and color of green tea (Camellia sinensis or C. assamica) leaves, J. Food Sci. Technol. 53 (2016) 721–729.
[48] P.P. Lewicki, E. Duszczyk, Color change of selected vegetables during convective air drying, Int. J. Food Prop. 1 (1998) 263–273.
[49] W. Zeng, D. Zhang, Y. Fang, J. Wu, J. Huang, Comparison of partial least square regression, support vector machine, and deep-learning techniques for estimating soil salinity from hyperspectral data, J. Appl. Remote Sens. 12 (2018) 022204.
[50] A.C. Burnett, J. Anderson, K.J. Davidson, K.S. Ely, J. Lamour, Q. Li, B.D. Morrison, D. Yang, A. Rogers, S.P. Serbin, A best-practice guide to predicting plant traits from leaf-level hyperspectral data using partial least squares regression, J. Exp. Bot. 72 (2021) 6175–6189.
[51] H. Feilhauer, G.P. Asner, R.E. Martin, S. Schmidtlein, Brightness-normalized partial least squares regression for hyperspectral data, J. Quant. Spectrosc. Radiat. Transf. 111 (2010) 1947–1957.
[52] C. Axelsson, A.K. Skidmore, M. Schlerf, A. Fauzi, W. Verhoef, Hyperspectral analysis of mangrove foliar chemistry using PLSR and support vector regression, Int. J. Rem. Sens. 34 (2013) 1724–1743.
[53] L. Gao, J. Li, M. Khodadadzadeh, A. Plaza, B. Zhang, Z. He, H. Yan, Subspace-based support vector machines for hyperspectral image classification, Geosci. Rem. Sens. Lett. IEEE 12 (2014) 349–353.
[54] B. Waske, S.v.d. Linden, J.A. Benediktsson, A. Rabe, P. Hostert, Sensitivity of support vector machines to random feature selection in classification of hyperspectral data, IEEE Trans. Geosci. Rem. Sens. 48 (2010) 2880–2889.
[55] J. Xia, J. Chanussot, P. Du, X. He, Rotation-based support vector machine ensemble in classification of hyperspectral data with limited training samples, IEEE Trans. Geosci. Rem. Sens. 54 (2016) 1519–1531.
[56] H. Meyer, E. Pebesma, Predicting into unknown space? Estimating the area of applicability of spatial prediction models, Methods Ecol. Evol. 12 (2021) 1620–1633.
[57] B. Takoutsing, G.B.M. Heuvelink, Comparing the prediction performance, uncertainty quantification and extrapolation potential of regression kriging and random forest while accounting for soil measurement errors, Geoderma 428 (2022) 116192.
[58] C. Adjorlolo, O. Mutanga, M.A. Cho, R. Ismail, Spectral resampling based on user-defined inter-band correlation filter: C3 and C4 grass species classification, Int. J. Appl. Earth Obs. Geoinf. 21 (2013) 535–544.
[59] V. Jain, A. Phophalia, Exponential weighted random forest for hyperspectral image classification, in: IGARSS 2019 - 2019 IEEE International Geoscience and Remote Sensing Symposium, 2019, pp. 3297–3300.
[60] E. Adam, H. Deng, J. Odindi, E.M. Abdel-Rahman, O. Mutanga, Detecting the early stage of phaeosphaeria leaf spot infestations in maize crop using in situ hyperspectral data and guided regularized random forest algorithm, Journal of Spectroscopy 2017 (2017) 6961387.
[61] J. Xia, W. Liao, J. Chanussot, P. Du, G. Song, W. Philips, Improving random forest with ensemble of features and semisupervised feature extraction, Geosci. Rem. Sens. Lett. IEEE 12 (2015) 1471–1475.
[62] M.C. Pasikatan, J.L. Steele, C.K. Spillman, E. Haque, Near infrared reflectance spectroscopy for online particle size analysis of powders and ground materials, J. Near Infrared Spectrosc. 9 (2001) 153–164.